2-7-2008

Structure, magnetic properties, and exchange coupling in thermally processed NdDyFeCoB/α-Fe nanoscale multilayer magnets

W. Liu
Chinese Academy of Sciences, Shenyang 110016, People's Republic of China

Xingzhong Li
University of Nebraska-Lincoln, xli2@unl.edu

Y. C. Sui
University of Nebraska - Lincoln

J. Zhou
University of Nebraska - Lincoln

W. J. Ren
Chinese Academy of Sciences, Shenyang 110016, People's Republic of China

See next page for additional authors

Structure, magnetic properties, and exchange coupling in thermally processed NdDyFeCoB/α-Fe nanoscale multilayer magnets

W. Liu,[1,2,a] X. Z. Li,[2] Y. C. Sui,[2] J. Zhou,[2] W. J. Ren,[1] Z. D. Zhang,[1] and D. J. Sellmyer[2]

[1]*Shenyang National Laboratory for Materials Science, Institute of Metal Research, and International Centre for Materials Physics, Chinese Academy of Sciences, Shenyang 110016, People's Republic of China*

[2]*Nebraska Center for Materials and Nanoscience and Department of Physics and Astronomy, University of Nebraska, Lincoln, Nebraska 68588-0113, USA*

(Presented on 9 November 2007; received 4 September 2007; accepted 29 October 2007; published online 7 February 2008)

The structure and magnetic properties of multilayer magnets with a hard phase (HP1 $=Nd_{13.5}Dy_{1.5}Fe_{68}Co_{10}B_7$ or HP2$=Nd_{14}Dy_1Fe_{68}Co_{10}B_7$) and soft phase Fe, prepared by sputtering and subsequent heat treatment, have been investigated. For Si/Ti(20 nm)/[HP1(2.0 nm)/Fe(0.5 nm)]$\times$200/Ti(10 nm) multilayer film, transmission electron microscopy results show that Fe disperses in amorphous NdDyFeCoB alloy. After annealing at 575 °C for 5 min, the hard $Nd_2Fe_{14}B$ phase typically with grains of about 50 nm and some amount of α-Fe coexist in the film. The grain size of the hard and soft phases can be controlled by the proper thickness of the layer and the period. A coercivity of 7.7 kOe and a ratio M_r/M_s of 0.74 are achieved in the multilayer Si/Ti(20 nm)/[HP2(2 nm)/Fe(0.5 nm)]$\times$200/Ti(10 nm). A good squareness of the hysteresis loop (measured even at 200 K) is observed, due to the effective exchange coupling between the magnetically soft and hard nanograins in the film. A pinning-type mechanism dominates the magnetization reversal process. In addition, the effect of the effective anisotropy, the grain size, and interfaces between the magnetically hard and soft phases on the exchange coupling is discussed. © *2008 American Institute of Physics*. [DOI: 10.1063/1.2834254]

Research on nanostructured exchange-coupled magnets has been performed since 1988.[1] Taking advantage of a high coercivity and a high magnetization provided by hard- and soft-magnetic components, respectively, a high remanence and a large maximum energy product would be obtained if a full and perfect exchange coupling existed between grains of the two phases in nanocomposite magnets, as predicted by micromagnetic calculations.[2–4] However, up to now, the energy products of rare-earth nanocomposite magnets prepared by means of rapid quenching and mechanical alloying have been much lower than the theoretical expectation, due to difficulties in controlling the nanostructures.[5–8] Recently, some studies on the exchange coupling were carried out for nanostructured CoSm/FeCo and PrCo/Co multilayers prepared by sputtering and subsequent heat treatment.[9,10] Magnetic properties of exchange-coupled α-Fe/Nd–Fe–B multilayer magnets were investigated by Shindo and Ishizone[11] and those for Nd–Fe–B/Fe/Nd–Fe–B trilayers were reported by Parhofer *et al.* and Yang and Kim.[12–14] In our previous study,[15] a high remanence of $J_r=1.31$ T and a relatively large maximum energy product of $(BH)_{max}=203$ kJ/m^3 (25.5 MGOe) were achieved in nanocomposite $(Nd,Dy)(Fe,Co,Nb,B)_{5.5}/\alpha$-Fe multilayer films on glass ceramic substrates.[15] Exchange coupling, structure, and magnetic properties of sputtered hard/soft multilayer magnets have been investigated.[16–20] In the present work, the Dy content of alloy target is reduced, while the thickness of both the hard and soft layers as well as the period of the multilayer is adjusted. The structure, magnetic properties, and exchange coupling in multilayer magnets are investigated in detail.

$(Nd,Dy)(Fe,Co,B)_{5.5}/\alpha$-Fe thin films were prepared with a multiple-gun dc- and rf-sputtering system by depositing HP1$=Nd_{13.5}Dy_{1.5}Fe_{68}Co_{10}B_7$ and HP2$=Nd_{14}Dy_1Fe_{68}Co_{10}B_7$ alloy and Fe onto silicon substrates, covered with a Ti buffer of 10 or 20 nm. The alloy target was made by sintering powdered compacts, while other targets were commercial products. The purities of all the targets were higher than 99.9%. The base pressure of the sputtering system was $(2-3)\times10^{-7}$ Torr, and the Ar pressure during the sputtering was 5 mTorr. The thickness of the films was measured by weighing samples. The substrate temperature was kept at room temperature with a water cooling system during sputtering. The as-deposited films were annealed in a furnace with a vacuum of 2×10^{-7} Torr. The crystalline structure of phases in the films was identified by x-ray diffractometry with Cu $K\alpha$ radiation, and by transmission electron microscopy (TEM). The magnetic properties of the films were measured by an alternating gradient force magnetometer (AGFM) and a superconducting quantum interference device (SQUID) magnetometer. The measuring field was applied in the plane of the film and the demagnetization coefficient was effectively zero.

Figures 1(a) and 1(b) show TEM bright-field images of the Si/Ti(20 nm)/[HP1(9 nm)/Fe(3 nm)]$\times$55/Ti(20 nm) multilayer film, where (a) and (b) are cross-section TEM images of the as-deposited multilayer film and that annealed at 575 °C for 5 min. From the cross-section view, the wide

[a]Author to whom correspondence should be addressed. Electronic mail: wliu@imr.ac.cn. FAX: 86-24-23893120.

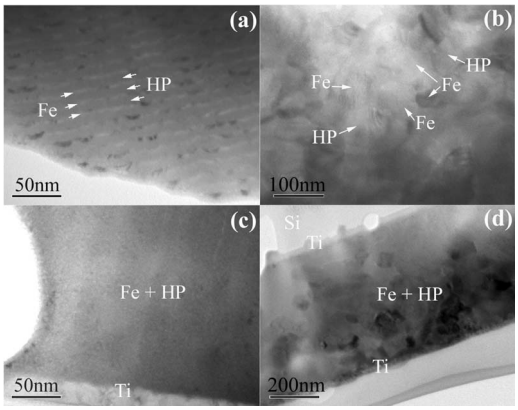

FIG. 1. TEM bright-field image of the Si/Ti(20 nm)/[HP1(9 nm)/Fe(3 nm)]×55/Ti(20 nm) and Si/Ti(20 nm)/[HP1(2.0 nm)/Fe(0.5 nm)]×200/Ti(20 nm) multilayer film, where (a) and (b), and (c) and (d) are cross-section TEM images of the former and latter deposited and annealed at 575 °C for 5 min, respectively.

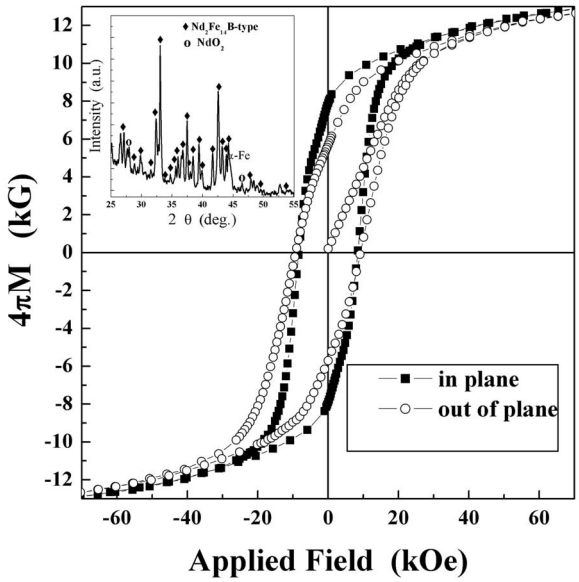

FIG. 2. Hysteresis loops at room temperature for the Si/Ti(20 nm)/[HP1(2.0 nm)/Fe(0.5 nm)]×200/Ti(20 nm) multilayer film annealed at 575 °C for 5 min and measured along the direction perpendicular and parallel to the film plane. The inset is XRD pattern of this multilayer film.

layer is amorphous NdDyFeCoB and the narrow one corresponds to Fe, similar to our previous work.[15] After annealing at 575 °C for 5 min, the grain sizes of $Nd_2Fe_{14}B$-type phase and α-Fe are close to 100 nm, as shown in Fig. 1(b). In order to control the size and distribution of the magnetically soft phase α-Fe, thinner Fe layers are deposited with more periods, as in the multilayer film Si/Ti(20 nm)/[HP1(2.0 nm)/Fe(0.5 nm)]×200/Ti(20 nm). Figures 1(c) and 1(d) give TEM bright-field image of the deposited and annealed multilayer films, respectively. It is seen from Fig. 1(c) that Fe disperses in the amorphous NdDyFeCoB alloy, due to very thin Fe layer in the multilayer film, which is different from Fig. 1(a) and the case of our previous work.[15] After annealing at 575 °C for 5 min, the hard $Nd_2Fe_{14}B$ phase typically with grains of about 50 nm and some amount of α-Fe coexist in the film [see Fig. 1(d)]. It is concluded that the grain size of the hard and soft phases can be controlled by the proper thickness of the layer and the period.

Figure 2 shows hysteresis loops at room temperature for the Si/Ti(20 nm)/[HP1(2.0 nm)/Fe(0.5 nm)]×200/Ti(20 nm) multilayer film annealed at 575 °C for 5 min and measured along directions perpendicular and parallel to the film plane, while the inset is its XRD pattern. It is found that the main magnetic phase is of the $Nd_2Fe_{14}B$ type, accompanied by some α-Fe and a trace of NdO_2. It is clear that the XRD peaks corresponding to $Nd_2Fe_{14}B$ type indicate random orientation, because the relative intensities of $Nd_2Fe_{14}B$-type phase are in agreement with those in the published x-ray diffraction data card obtained from a randomly oriented powder. The hysteresis loop parallel to the film plane shows that a coercivity of 8.5 kOe and a ratio M_r/M_s of 0.62 are observed in the nanocomposite film. The difference of the remanences measured along the directions perpendicular and parallel to the film plane is due to different demagnetization factors in the two directions. If the demagnetization factor were taken into account, the hysteresis loops of the multilayer film would be isotropic.

In order to enlarge the effective exchange length, we reduce the anisotropy of the hard phase by decreasing the Dy content in the alloy. XRD patterns for as-deposited (Si substrate)/Ti(20 nm)/[HP2(2 nm)Fe(0.5 nm)]×200/Ti (10 nm) multilayers annealed at 600 °C for 1 min and at 575 °C for 30 min are shown in Fig. 3. It can be seen that the as-deposited multilayer film is amorphous. After annealing at 600 °C for 1 min, the main magnetic phase of $Nd_2Fe_{14}B$ type and a trace of NdO_2 are observed in the film. It is hard to observe α-Fe due to the short annealing time and thin Fe layers in the multilayer film. However, for thicker Fe layers, short annealing time also leads to the appearance of α-Fe in the multilayer film.[19] By contrast, annealing at 575 °C for 30 min shows that the α-Fe phase is clearly observed in the film. It is concluded that two phases can be obtained by means of an appropriate annealing conditions, even if the Fe layers are very thin in the multilayer film.

Figure 4(a) gives hysteresis loops at room temperature of the single layer (Si substrate)/Ti(20 nm)/[HP2(400 nm)]/

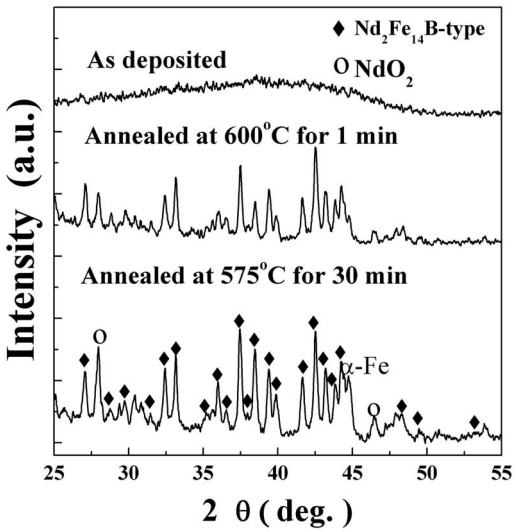

FIG. 3. XRD patterns for as-deposited (Si substrate)/Ti(20 nm)/[HP2(2 nm)Fe(0.5 nm)]×200/Ti(10 nm) multilayers annealed at 600 °C for 1 min and at 575 °C for 30 min.

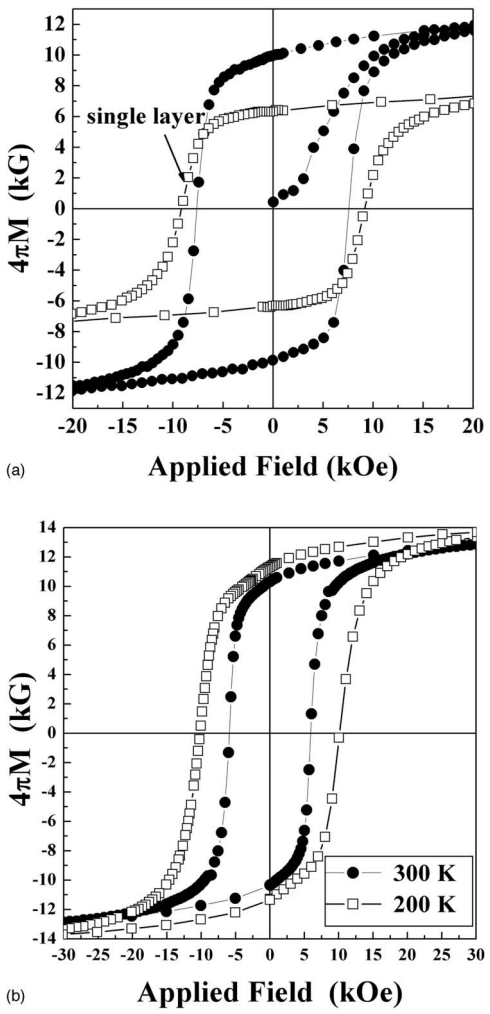

FIG. 4. (a) Hysteresis loops at room temperature of the single layer (Si substrate)/Ti(20 nm)/[HP2(400 nm)]/Ti(10 nm) and Si (substrate)/Ti(20 nm)/[HP2(2 nm)Fe(0.5 nm)]×200/Ti(10 nm) multilayer film annealed at 600 °C for 1 min. (b) Hysteresis loops at room temperature and at 200 K for Si (substrate)/Ti(20 nm)/[HP2(2 nm)Fe(0.5 nm)]×200/Ti(10 nm) multilayer film annealed at 575 °C for 30 min.

Ti(10 nm) and Si (substrate)/Ti(20 nm)/[HP2(2 nm)Fe(0.5 nm)]×200/Ti(10 nm) multilayer film annealed at 600 °C for 1 min. In comparison with the remanence of the single layer ($4\pi M_r$=6.3 kG), the multilayer remanence is enhanced to 9.9 kG. Also, a coercivity of 7.7 kOe, a maximum energy product of 20 MGOe and M_r/M_s of 0.74 are achieved in the multilayer film. It is seen from the initial magnetization curve at room temperature of the nanocomposite film that a pinning-type mechanism dominates the magnetization reversal process. In addition, more periods of the layers of hard and soft phases are present, which leads to more interfaces between hard and soft phases; these may act as pinning centers, which is consistent with a higher intrinsic coercivity. Figure 4(b) shows hysteresis loops at room temperature and at 200 K for Si (substrate)/Ti(20 nm)/[HP2(2 nm)Fe(0.5 nm)]×200/Ti (10 nm) multilayer film annealed at 575 °C for 30 min. At room temperature, an intrinsic coercivity of 5.8 kOe and a maximum energy product of 18.8 MGOe are observed in the multilayer film. A good squareness of the hysteresis loop (measured even at 200 K) is observed, due to the effective exchange coupling between the magnetically soft and hard nanograins in the film, although the effective anisotropy is enhanced at low temperature. This suggests that the exchange length is enlarged due to the decrease of effective anisotropy and the grain size of the soft phase is reduced due to the decrease in thickness of hard and soft phases in the nanocomposite film.

In summary, we prepared nanocomposite film magnets containing an $Nd_2Fe_{14}B$-type hard phase and Fe by sputtering and subsequent heat treatment. It is concluded that the grain size of the hard and soft phases can be controlled by choosing the proper thickness of the layers and period. The magnetic measurements at low temperature suggest that the exchange length is enlarged and the grain size of the soft phase are reduced by the decrease of the anisotropy field of the hard phase and the reduction of thickness of hard and soft phase layers, respectively. The reduction of the Dy content leads to a reduction of the coercivity. On the other hand, more interfaces between hard and soft phases result in the enhancement of the intrinsic coercivity in nanocomposite films.

Research at Nebraska has been supported by the U.S. DOE under Grant No. DE-FG02-04ER46152, with infrastructure support from the Nebraska Center for Materials and Nanoscience. The work in China was supported by the National Natural Science Foundation of China under Project Nos. 50331030 and 50571098. One of authors (W.J.R.) gratefully acknowledges the support of K. C. Wong Education Foundation, Hong Kong.

[1] R. Coehoorn, D. B. de Mooji, and C. D. E. Waard, J. Magn. Magn. Mater. **80**, 101 (1989).
[2] R. Skomski and J. M. D. Coey, Phys. Rev. B **48**, 15812 (1993).
[3] T. Schrefl, H. Kromüller, and J. Fidler, J. Magn. Magn. Mater. **127**, L237 (1993).
[4] E. F. Kneller and R. Hawig, IEEE Trans. Magn. **27**, 3588 (1991).
[5] J. Ding, P. G. McCormick, and R. Street, J. Magn. Magn. Mater. **124**, 1 (1993).
[6] A. Manaf, R. A. Buckley, and H. A. Davies, J. Magn. Magn. Mater. **128**, 302 (1993).
[7] L. Withanawasam, A. S. Hurphy, G. C. Hadjipanayis, and R. F. Krause, J. Appl. Phys. **76**, 7065 (1994).
[8] X. K. Sun, J. Zhang, Y. L. Chu, W. Liu, B. Z. Cui, and Z. D. Zhang, Appl. Phys. Lett. **74**, 1740 (1999).
[9] I. A. Al–Omari and D. J. Sellmyer, Phys. Rev. B **52**, 3441 (1995).
[10] J. P. Liu, Y. Liu, R. Skomski, and D. J. Sellmyer, IEEE Trans. Magn. **35**, 3241 (1999).
[11] M. Shindo and M. Ishizone, J. Appl. Phys. **81**, 4444 (1997).
[12] S. Parhofer, J. Wecker, C. Kuhrt, and G. Gieres, IEEE Trans. Magn. **32**, 4437 (1996).
[13] S. Parhofer, G. Gieres, J. Wecker, and L. Schultz, J. Magn. Magn. Mater. **163**, 32 (1996).
[14] C. J. Yang and S. W. Kim, J. Magn. Magn. Mater. **202**, 311 (1999).
[15] W. Liu, Z. D. Zhang, J. P. Liu, L. J. Chen, L. L. He, Y. Liu, X. K. Sun, and D. J. Sellmyer, Adv. Mater. (Weinheim, Ger.) **14**, 1832 (2002).
[16] W. Liu, Z. D. Zhang, J. P. Liu, X. Z. Li, X. K. Sun, and D. J. Sellmyer, J. Appl. Phys. **91**, 7890 (2002).
[17] W. Liu, Z. D. Zhang, J. P. Liu, Z. R. Dai, Z. L. Wang, X. K. Sun, and D. J. Sellmyer, J. Phys. D **36**, L63 (2003).
[18] W. Liu, Z. D. Zhang, J. P. Liu, B. Z. Cui, X. K. Sun, J. Zhou, and D. J. Sellmyer, J. Appl. Phys. **93**, 8131 (2003).
[19] W. Liu, X. Z. Li, J. P. Liu, X. K. Sun, C. L. Chen, R. Skomski, Z. D. Zhang, and D. J. Sellmyer, J. Appl. Phys. **97**, 104308 (2005).
[20] W. Liu, Y. C. Sui, J. Zhou, X. K. Sun, C. L. Chen, Z. D. Zhang, and D. J. Sellmyer, J. Appl. Phys. **97**, 10K303 (2005).